

ENHANCEMENT OF THIRD-ORDER OPTICAL NONLINEARITIES IN 72GeS₂-18Ga₂S₃-10CdS GLASSES BY Ag ION IMPLANTATION

M. SONG, Q. M. LIU*, G. XU CAI, F. REN

School of Physics and Technology, Key Lab of Artificial Micro- and Nano-structures of Ministry of Education, Wuhan University, Wuhan 430072, P. R. China

The third-order nonlinearity of 72GeS₂-18Ga₂S₃-10CdS chalcogenide glass implanted by Ag ions was studied. The doses for implantation were ranging from 1×10^{16} to 2×10^{17} ions/cm² and Ag nanoparticles were observed by the AFM measurements. The third-order nonlinear optical property $\chi^{(3)}$ was measured by the femtosecond Z-scan technique and showed the maximum value of 7.58×10^{-11} esu. The results indicated that the $\chi^{(3)}$ enhancement of implanted samples was due to the formation of Ag nanoparticles. The relation between the implanted dose and the third order nonlinearity was related to the enhancement of local field inside the particles and the interaction between Ag nanoparticles, which will be useful in fabricating optical devices by controlling the implanted doses to controlling the optical nonlinearity in glasses.

(Received July 6, 2015; Accepted September 11, 2015)

Keywords: Chalcogenide glass; Ion implantation; Third-order nonlinearity

1. Introduction

Amorphous chalcogenide glasses based on the chalcogen elements S, Se, Te have attracted many scientists interest on the fundamental researches due to their formation, structure and properties [1-3]. Especially for high refractive index, large optical nonlinear susceptibility, high and wide transmission in visible and near-IR region [4], it has many potential applications in photonics and nonlinear optics. Metal nanoparticles composite glasses have been intensively studied due to their improvement of third-order nonlinearities and ultrafast time response in the surface plasmon resonance absorption region [5]. Recently, the methods of metallic nanoparticles synthesis contained: Sol-Gel technology[6-7], pulsed laser irradiation[8], plasma-enhanced chemical vapour deposition (PECVD)[9], ion exchange[10] and ion implantation so on. Compared to other methods, ion implantation is the most versatile of the mechanical methods to implant nanoparticles into glasses [11]. It has many advantages like easy fabrication of any combination of metal-dielectric controlling on the concentration of the implanted impurity and the spatial location of the ion beam on sample, but the influence of ion implantation process on the growth of nanoparticles is complicated. It is mostly used to modify transparent matrixes like silica and other oxide matrixes, which induces the formation of metal nanoparticles inside the matrix [12]. However, to the best of our knowledge, there is little research on metal nanoparticles embedded in chalcogenide glasses by ion implantation expect our work before [5]. So, it is necessary for us to

*Corresponding author : qmliu@whu.edu.cn

study on this field, finding a new candidate material for optoelectronic devices. In this paper, homogeneous bulk $72\text{GeS}_2\text{-}18\text{Ga}_2\text{S}_3\text{-}10\text{CdS}$ glasses were prepared by the traditional melt-quenching technique. Ag nanoparticles were formed by implanting Ag ions in the $72\text{GeS}_2\text{-}18\text{Ga}_2\text{S}_3\text{-}10\text{CdS}$ glasses. The third-order optical nonlinearities were measured by the Z-scan technique. Also, the influence of the dose on $\chi^{(3)}$ was discussed.

2. Experiments

Homogeneous bulk $72\text{GeS}_2\text{-}18\text{Ga}_2\text{S}_3\text{-}10\text{CdS}$ glasses were prepared by the melt-quenching technique from high purity Ge, Ga, S and CdS. The substrate samples were cut from the bulk glasses with 10 mm in diameter and 1 mm in thickness, which were polished to optical grade on both sides for further experiment. Ag ions with an energy of 70KeV were implanted into $72\text{GeS}_2\text{-}18\text{Ga}_2\text{S}_3\text{-}10\text{CdS}$ substrates, placed in a vacuum with various dose of 1×10^{16} , 3×10^{16} , 5×10^{16} , 1×10^{17} and 2×10^{17} ions/cm² by the metal vapor vacuum arc ion source (MEVVA) implanter at room temperature.

Optical transmittance spectra were characterized by a UV-Vis dual-beam spectrophotometer (Analytikjena, SPECORD 210 PLUS) with wavelengths from 300 to 1100 nm at room temperature. The refractive index n_0 was measured in Spectroscopic ellipsometer (TP-77) in the wavelength range of 500-900 nm. The surface morphology of chalcogenide glass implanted was observed by AFM (SPM-9500J3 SHIMADZU).

The third-order optical nonlinear properties of all samples were characterized by using the standard Z-Scan method. The excitation source is a mode-locked Ti: sapphire laser (Coherent, Mira 900), with a pulse duration of 150fs and a repetition rate of 76 MHz. 700 nm wavelength was used for excitation in the experiment. The laser pulses were focused onto samples by a lens of 150 mm focal length. The radius of the Gaussian beam spot at focal waist ω_0 is 4.34 mm. The input irradiance used here was kept at 4.708 GW/cm^2 . Sample was gradually moved along the propagation direction of the Gaussian beam under the control of a PC. The transmitted laser power was monitored by a detector, and the signals were recorded by a computer. Open- and closed-aperture Z-Scans of each sample were performed to study the nonlinear refraction and nonlinear absorption.

3. Result and discussion

Fig. 1 shows the optical transmittance spectra of Ag implanted samples with doses ranging from 1×10^{16} to 2×10^{17} ions/cm² at the energy of 70 KeV. The optical transmittance spectrum of the host glass was also shown for comparison in Fig.1. The host glass showed a high transmittance about 80% at the laser wavelength of 700 nm. The cutting-off absorption edge was in 450 nm. The transmittance of the implanted samples declined with the increasing of dose, which indicated the formation of Ag nanoparticles, despite the SPR absorption peaks was not observed[12]. The saltation at 820 nm comes from the instrument error. With the increasing of Ag ion dose implanted, the optical transmittance spectra were red shifted, which indicated the size of Ag nanoparticles

increased, but the increased transmittance at the dose of 2×10^{17} ions/cm² would be attributed to the minus reflection features of Ag particles, which was also related to the size of particle[14].

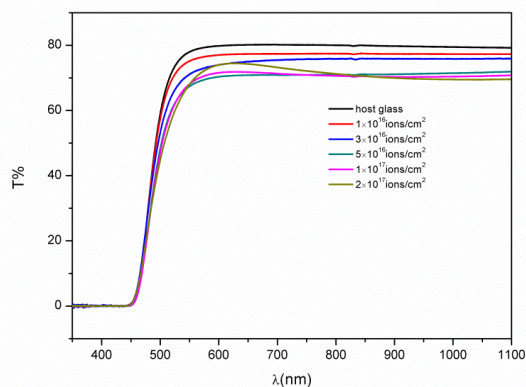


Fig.1. The transmittance spectra of Ag implanted samples with various dose and host glass

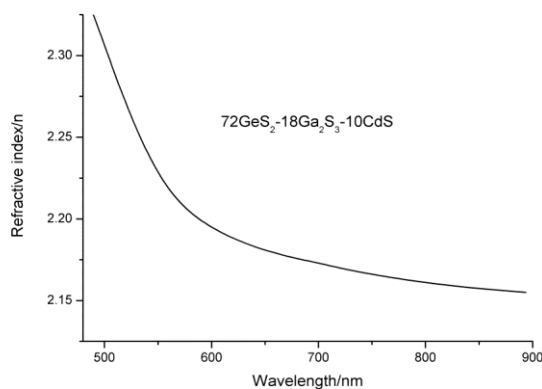


Fig.2. The refractive index of $72\text{GeS}_2\text{-}18\text{Ga}_2\text{S}_3\text{-}10\text{CdS}$ glasses.

The linear refractive of $72\text{GeS}_2\text{-}18\text{Ga}_2\text{S}_3\text{-}10\text{CdS}$ glasses varied as a function of wavelength at 500-900 nm is shown in Fig.2. They followed the typical dispersion curve of chalcogenide glasses.

The surface morphology of the implanted samples was observed by AFM (as shown in Fig.3).

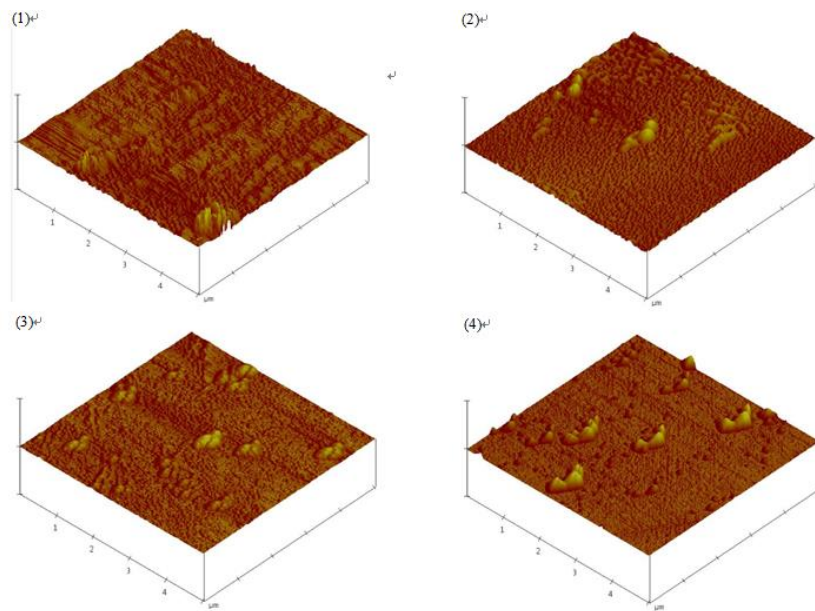


Fig.3. AFM images of $72\text{GeS}_2\text{-}18\text{Ga}_2\text{S}_3\text{-}10\text{CdS}$ glasses implanted with the dose of 3×10^{16} ions/cm² (1), 5×10^{16} ions/cm² (2), 1×10^{17} ions/cm² (3), 2×10^{17} ions/cm² (4)

As shown in Fig.3, Ag nanoparticles were formed in the implanted $72\text{GeS}_2\text{-}18\text{Ga}_2\text{S}_3\text{-}10\text{CdS}$ glasses. The nanoparticles appear irregular hemisphere shape. The size of sample implanted with the dose of 1×10^{16} ions/cm² was about 90 nm, which was obtained from Fig.4. With the increase of implanted dose, the sizes of nanoparticles increase, which was recorded in Table.1.

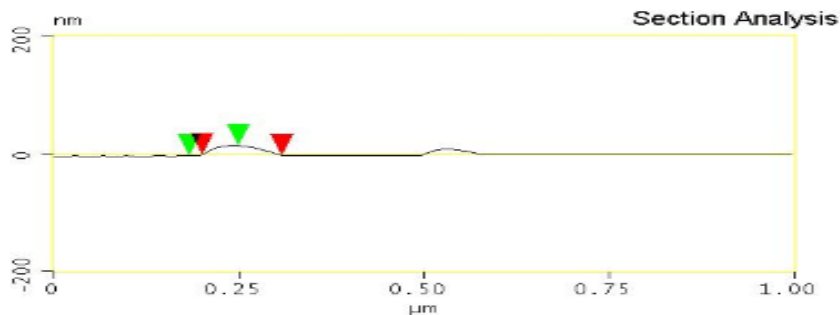


Fig.4. The single nanoparticle size of size of sample implanted with the dose of 1×10^{16} ions/cm²

The femtosecond Z-scan experiments were performed to record the Open- and closed-aperture signal of 70 KeV Ag implanted samples at different doses and the substrate. Take the sample implanted at the dose of 1×10^{17} ions/cm² as an example (as shown in Fig.5). From the shape of the normalized transmittance $T(z)$ (shown in Fig.5a), we can determine the sign of the nonlinear absorption (NLA) coefficient β . A dip in the z-scan curve around the focal position ($z = 0$) implies a decrease in transmission, which indicates that the sample possess the characteristic of positive nonlinear absorption coefficient ($\beta > 0$) and reverse saturable absorption [15]. Also, the sign of the nonlinear refractive (NLR) index γ can be confirmed. The closed aperture data should be divided by the open-aperture data [15-17]. As shown in Fig.5b the valley-peak patterning (a prefocal transmittance valley followed by a postfocal transmittance maximum) indicates the

positive sign of the NLR index ($\gamma > 0$), and the self-focusing properties of the sample [13].

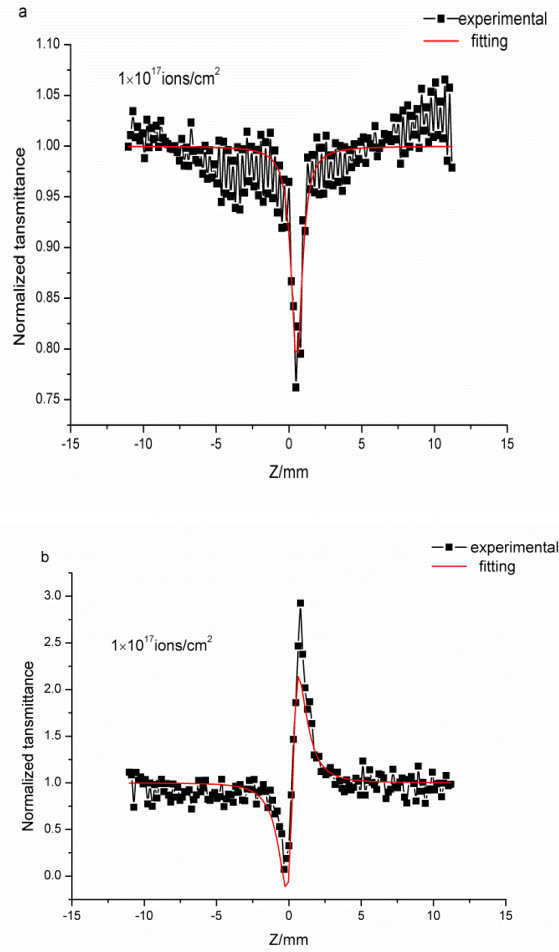


Fig.5. The Open-aperture profile (a) and closed-aperture profile (b) of the samples implanted with the dose of 1×10^{17} ions/cm². The square and solid curve implies the experiment value and its simulation, respectively.

The effective NLA coefficient β and the NLR index γ can be calculated by the following relationships [18]

$$T_{OA} = \sum_{m=0}^{\infty} \frac{(-q_0)^m}{(1 + z^2/z_0^2)^m (1+m)^{3/2}} \quad (1)$$

$$\frac{T_{CA}}{T_{OA}} = 1 + \frac{4\Delta\phi_0 z/z_0}{[(z/z_0)^2 + 9][(z/z_0)^2 + 1]} \quad (2)$$

Where $q_0 = \beta I_0 L_{eff}$, $\Delta\phi_0 = \gamma k I_0 L_{eff}$, $\alpha = -\ln(p'/p_0)/L$, I_0 is the peak irradiance at the focus ($z=0$). L_{eff} is the effective thickness of the samples, $k = 2\pi/\lambda$ is the wave vector of the laser radiation, z_0 is the Rayleigh length of the Gaussian incident beam. While the relations between

third-order nonlinear susceptibility $\chi^{(3)}$ and β, γ are list in the follow equations [15]:

$$\chi^{(3)} = \chi_{\text{Re}}^{(3)} + i\chi_{\text{Im}}^{(3)}$$

$$\chi_{\text{Re}}^{(3)} = 2n_0^2 \varepsilon_0 c \gamma \tag{3}$$

$$\chi_{\text{Im}}^{(3)} = \frac{n_0^2 \varepsilon_0 c \lambda \beta}{2\pi} \tag{4}$$

Therefore, the absolute values of third-order nonlinear susceptibility can be written as:

$$\chi^{(3)} = \sqrt{\left(\chi_{\text{Re}}^{(3)}\right)^2 + \left(\chi_{\text{Im}}^{(3)}\right)^2} \tag{5}$$

The solid curve of Open- and closed-aperture in Fig.5 are fitted by employing Eq.(1) and (2), respectively. The Open- and closed-aperture simulation values of all samples are recorded in Fig.6. After fitting the data, we got the values of the effective NLA coefficient β and the NLR index γ . Then the value of $\chi^{(3)}$ for all samples can be obtained by Eqs. (3), (4) and (5). The third-order nonlinearity values of all samples were recorded in Table.1.

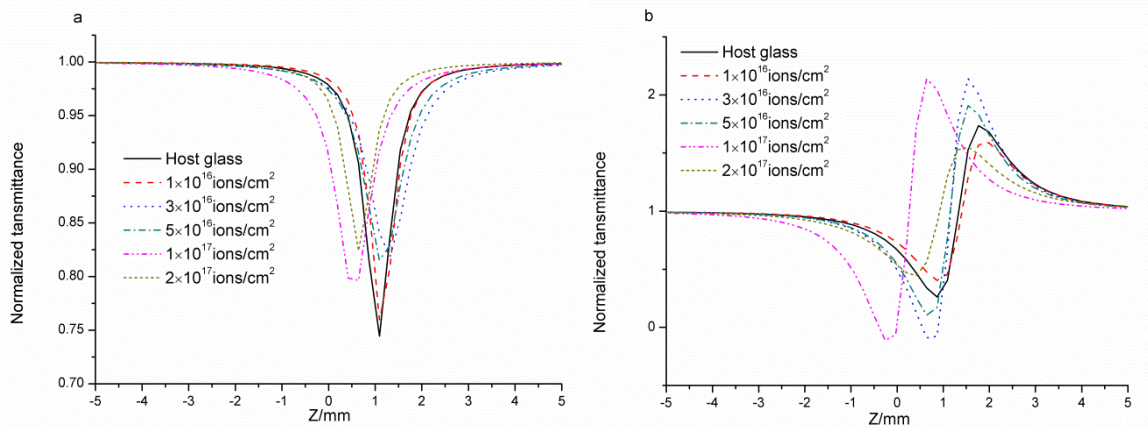


Fig.6. The Open-aperture simulation profile (marked a) and closed-aperture simulation profile (marked b) of all samples.

Table.1.The third-order nonlinearity results of all samples

	substrate	1×10^{16}	3×10^{16}	5×10^{16}	1×10^{17}	2×10^{17}
$\chi^{(3)}$ (10^{-11} esu)	1.39	1.58	4.83	5.70	7.58	2.87
Nanoparticles Size (nm)	0	~90	~150	~200	~250	~300

From the recorded data above, we can see that the magnitude of $\chi^{(3)}$ was enhanced after ion implantation, and it shows the trend of increasing firstly and then decreasing with the doses, reaching its maximum 7.58×10^{-11} esu at the dose of 1×10^{17} ions/cm². That is to say the 1×10^{17} ions/cm² dose is the optimum dose to obtain the best optical property in our experiments. The third-order nonlinearity of metal nanoparticles contained composite glasses depends mainly on the

electronic effects of metal nanoclusters, which contains intraband and interband transitions. The earlier researcher found that the appearance of surface plasmon resonance (SPR) strongly enhances the optical property by the enhancement of local field inside the particle [19-20]. It is well known that the surface plasmon resonance (SPR) absorption is size-dependent for nanoparticles. When the nanoparticle is less than 60 nm, there is only one peak in the absorption spectra. When the size of nanoparticles becomes larger, higher polarization resonance like quadrupole or octupole resonance occurs, which induces the SPR of higher polarization [12]. The obvious absorption peak at 500 nm and the red shifted of optical transmittance spectra indicated that the increasing of the size of Ag nanoparticles could origin from it. By using the Maxwell garnett theory, the local field inside the particle is given by

$$E_1 = \frac{3\varepsilon_d}{\varepsilon_m + 2\varepsilon_d} E_0 = fE_0$$

Where ε_m and ε_d refer to the dielectric functions of the metal particles and the dielectric host, respectively. E_0 is the incident electric field, and f is the local field factor. When $\varepsilon_m + 2\varepsilon_d$ reach a minimum, SPR occurs, and the nonlinear polarization reach a maximum. In nanocomposites, the relation between $\chi_{eff}^{(3)}$ and $\chi_m^{(3)}$ is $\chi_{eff}^{(3)} \propto p |f|^2 f^2 \chi_m^{(3)}$, where p is the volume fraction of metal particles. $\chi_{eff}^{(3)}$ and $\chi_m^{(3)}$ are the third-order nonlinear susceptibility of composite and metal material, respectively [10,21]. Therefore the enhancement of third order nonlinearity after ion implantation depends on the increase of the volume fraction of Ag nanoparticles. However, when the volume fraction got larger, the quantum effect weakened and the electromagnetic interactions between particles became stronger, which showed side effects on the enhancement of third order nonlinearity [13]. The third-order nonlinear susceptibility reaches a maximum at the dose of 1×10^{17} ions/cm², which could be attributed to the change of the size-dependent volume fraction of Ag nanoparticles in 72GeS₂-18Ga₂S₃-10CdS glasses with different ion implanted doses.

4. Conclusions

In this paper, Ag nanoparticles were fabricated in 72GeS₂-18Ga₂S₃-10CdS chalcogenide glasses by ion implantation. The enhancement of third-order nonlinear optical properties of the implanted samples was due to the formation of Ag nanoparticles. The values of $\chi^{(3)}$ have the trend of increasing firstly and then decrease with the dose, the maximum $\chi^{(3)} 7.58 \times 10^{-11}$ esu at the dose of 1×10^{17} ions/cm² was obtained. We thought that this phenomenon was attributed to the enhancement of local field inside the particle and the interaction between Ag nanoparticles.

Acknowledgments

This research work was financially supported by the National Natural Science Foundation of China (51272183 and 51572202) and the Nanotechnology Program of Suzhou (ZXG201438).

References

- [1] A. B. Seddon, *Journal of Non-Crystalline Solids*. **184**, 44 (1995).
- [2] Vahid G. Ta'eed, Neil J. Baker, Libin Fu, Klaus Finsterbusch, Michael R.E. Lamont, David J. Moss, Hong C. Nguyen, Benjamin J. Eggleton, Duk Yong Choi, Steven Madden, B. Luther-Davies, *OPTICS EXPRESS*. **15**, 9205 (2007).
- [3] Q. M. Liu and P. Zhang, *Sci Rep*. **4**, 5719 (2014).
- [4] Q. M. Liu, B. Lu, X. J. Zhao, F. X. Gan, J. Mi, and S. X. Qian, *Journal of Non-Crystalline Solids*. **351**, 3147 (2005).
- [5] Q. M. Liu, X. He, X. J. Zhao, F. Ren, X. H. Xiao, C. Z. Jiang, X. Zhou, L. Lu, H. Zhou, S. Qian, B. Poumellec, and M. Lancry, *Journal of Nanoparticle Research*. **13**, 3693 (2011).
- [6] S. Otsuki, K. Nishio, T. Kineri, Y. Watanabe, and T. Tsuchiya, *Journal of the American Ceramic Society*. **82**, 1676 (1999).
- [7] E. Borsella, M. Falconieri, S. Botti, S. Martelli, F. Bignoli, L. Costa, S. Grandi, Luigi Sangaletti, B. Allieri, and L. Depero, *Materials Science and Engineering: B*. **79**, 55 (2001).
- [8] Y. Dai, H. L. Ma, B. Lu, B. K. Yu, B. Zhu, and J. R. Qiu, *OPTICS EXPRESS*. **16**, 3912 (2008).
- [9] G. V. Prakash, M. Cazzanelli, Z. Gaburro, L. Pavesi, F. Iacona, G. Franzo, and F. Priolo, *Journal of Modern Optics*. **49**, 719 (2002).
- [10] X. C. Yang, Z. H. Li, W. J. Li, J. X. Xu, Z. W. Dong, and S. X. Qian, *Chinese Science Bulletin*. **53**, 695 (2008).
- [11] Daven Compton, Lesley Cornish, and E. v. d. Lingen, *Gold Bulletin*. **36**, 10 (2003).
- [12] F. Ren, C. Z. Jiang, C. Liu, J. B. Wang, and T. Oku, *Phys Rev Lett*. **97**, 165501 (2006).
- [13] Q. M. Liu, X. He, X. Zhou, F. Ren, X. H. Xiao, C. Z. Jiang, H. Zhou, X. J. Zhao, L. P. Lu, and S. X. Qian, *Journal of Non-Crystalline Solids*. **357**, 2320 (2011).
- [14] T. Han, S. Zhang, J. Q. Wang, X. M. Cheng, *Acta Phys. Sin.* **60**, 27303 (2011).
- [15] Y. H. Wang, C. Z. Jiang, F. Ren, Q. Q. Wang, D. J. Chen, and D. J. Fu, *Journal of Materials Science*. **42**, 7294 (2007).
- [16] M. Sheik-Bahae, D. J. Hagan, and E. W. Van Stryland, *Phys Rev Lett*. **65**, 96 (1990).
- [17] M. Sheik-Bahae, A. A. Said, T.-H. Wei, D. J. Hagan, and E. W. Van Stryland, *Quantum Electronics*. **26**, 760 (1990).
- [18] H. M. Gong, Z. K. Zhou, S. Xiao, H. Song, X. R. Su, M. Li, and Q. Q. Wang, *Chinese Physics Letters*. **24**, 3443 (2007).
- [19] G. Battaglin, E. Cattaruzza, G. De Marchi, F. Gonella, G. Mattei, C. Maurizio, P. Mazzoldi, M. Parolin, C. Sada, and I. Calliari, *Nuclear Instruments and Methods in Physics Research B*. **191**, 392 (2002).
- [20] E. Cattaruzza, G. Battaglin, P. Calvelli, F. Gonella, G. Mattei, C. Maurizio, P. Mazzoldi, S. Padovani, R. Polloni, C. Sada, B. F. Scremin, and F. D'Acapito, *Composites Science and Technology*. **63**, 1203 (2003).
- [21] D. Ricard, Ph. Roussignol, and C. Flytzanis, *OPTICS LETTERS*. **10**, 511 (1985).